Article

Journal of the Brazilian Chemical Society

https://dx.doi.org/10.21577/0103-5053.20240154

J. Braz. Chem. Soc. **2025**, *36*, 3, e-20240154, 1-11

Mechanical and Thermal Properties of Poly (Butylene Adipate-*co*-Terephthalate) / Poly (Lactic Acid) Blend and Montmorillonite Functionalized by Ionic Liquids Composites

Renata S. Dias,[a] Fernando R. Scremin,[b,c] Paulo R. S. Bittencourt,[a] Douglas C. Dragunski,[b] Alex S. Torquato[a] and Oldair D. Leite *,[a]

[a]*Departamento Acadêmico de Química, Universidade Tecnológica Federal do Paraná, 85722-332 Medianeira-PR, Brazil*

[b]*Centro de Engenharias e Ciências Exatas, Universidade Estadual do Oeste do Paraná, 85903-000 Toledo-PR, Brazil*

[c]*Departamento de Química, Instituto Federal do Paraná, Campus Umuarama, 87507-014 Umuarama-PR, Brazil*

The composites of poly (butylene adipate *co*-terephthalate) / poly (lactic acid) (PBAT/PLA) blend and montmorillonites functionalized using imidazole-derived ionic liquids with different carbon chain sizes (butyl, octyl, and dodecyl) proved to be a promising alternative for improving the thermal and mechanical properties of the polymer blend. Functionalization of montmorillonites by ionic liquids was confirmed by increasing the basal spacing, and spectroscopical and thermal analysis evidence. The composite synthesis was carried out by casting technique generating homogeneous polymeric films. X-ray diffraction analyses suggested that montmorillonite functionalization with the ionic liquid of the butyl carbon chain fostered exfoliation and incorporation of the clay into the polymer. Furthermore, an increase in the thermal stability and mechanical properties of the material was observed. The other composites formed between the PBAT/PLA blend and the montmorillonite functionalized by ionic liquids of higher carbonic chain showed micro composites formation. Thus, their thermal and mechanical properties had no significant improvements.

Keywords: ionic liquids, functionalization of clays, exfoliation

Introduction

Natural and artificial polymers have the potential for advancement in materials science by copolymerization and alternatives blends, expanding their application. Also on the rise are biodegradable polymers and their blends from renewable and other sources since they are considered environmentally favorable as they are broken down by microorganisms, linked to their chemical structure and not to the raw material.[1,2]

The biodegradable polymer blend obtained by incorporating the renewable polyester poly (lactic acid) (PLA) with the petroleum-derived polymer poly (butylene adipate *co*-terephthalate) (PBAT) illustrates the possibility of modulating properties of the final material as a function of the ratios of each polymer could be achieved. In this blend the low flexibility and thermal resistance of PLA are compensated by the high elasticity and wear and fracture resistance of PBAT and the low tensile strength of PBAT by the high PLA mechanical strength.[3] The blend applied in this study has been marketed since 1990 under the trading name Ecovio®, serving mainly the packaging sector.

In addition to its efficient stiffness reduction, PBAT/PLA blends properties may be optimized by incorporating fillers that improve thermal stability, biodegradation rate, especially in nanometric systems.[4] In polymeric nanocomposites, the properties transferring between materials depend on the nanoscale dynamics of the fillers, differing from micro composites. Thus, thermoplastic polymers, thermosets, or elastomers are linked to nanoparticles such as clays and carbon nanotubes, creating a new material where the influence of particle size and their degree of interaction are determinants of the final properties.[5,6]

Bentonite clays, such as montmorillonite (MMT), have been applied in polymers compositions due to their size

*e-mail: oldair.leite@gmail.com
Editor handled this article: Rodrigo A. A. Muñoz (Associate)

and high surface area, thermal and frictional resistance, high cation exchange capacity, delamination, swelling and adsorption, plasticity, rheological properties, availability, and affordability.[7,8] Organophilized clays, as polymer matrix fillers, add superior final mechanical behavior to the polymer;[6] good thermostability;[9] substantial tensile strength increases;[7] matrix stiffness without reducing its fracture behavior;[10] and significant gains for gas barrier properties and modulus of elasticity.[1]

The silicate/polymer nanocomposite final properties depend on the degree of the polymer/clay interaction, requiring processing of the natural material, such as purification, activation, and surface chemical modification.[11,12] This step of the process, called functionalization, aims to make the clay and polymer compatible, changing the surface of the natural inorganic material to organophilic and compatible with the polymer matrix by chemical processes.[13] Cation exchange with organic solvents is the predominant method adopted, varying the modification method, organic solvent, and its proportion, affecting the final properties.[14,15]

Organic molecules contain groups that can interact with the exchangeable cation on the MMT surface, acting as hydrophobic surfactants, organophilizing the clay and increasing its spacing to interact with polymers.[16] Quaternary ammonium salts, non-ionic surfactants, ionic surfactants, and ionic liquids are alternatives to organic solvents.[14,17]

Ionic liquids (ILs) are organic salts with fusion temperature below 100 °C and attractive solvent characteristics due to their multifunctional structure: one "apolar part" respective to the alkyl chain; and another polar, such as the imidazolium cation, as in this study; that allows affinity to organic and inorganic materials, facilitating polymerization and phase interaction. Solubility, greater ability to control hydrophilic balance, amphiphilic material processability, low volatility, and lack of flammability that ensure superior thermal properties are other advantages of the ILs.[18] For its green and environmentally favorable solvent characteristic, studies are advancing the understanding of its effects on the final properties of the clays and polymer composites.[12]

This study aimed to evaluate new behaviors of thermal, mechanical, and structural properties of new composites produced from PBAT/PLA blends and natural MMT functionalized with imidazolium-derived ionic liquids synthesized with different carbon chains.

Experimental

The natural montmorillonite (MMT) used is from a deposit located in the municipality of Pedra Lavrada, PB, Brazil. Its physical-chemical properties are not cataloged since it is not a commercial material. Its appearance is reminiscent of a fine grayish powder without agglomerates or visible contaminants. The particle size distribution curve of the natural sample describes an average particle diameter of 18.73 μm.

Based on the thermogravimetric and structural characterization by X-ray diffractometry of the clay, thermal activation of the clay was carried out to remove any volatile contaminants by calcination at 250 °C for 8 h and cooling to room temperature (25 °C) in a desiccator. The cation exchange capacity (CEC) of natural MMT was determined following the ASTM C837-84 (Standard Test Method for Methylene Blue Index of Clay), obtaining a CEC of 40 mEq 100 g^{-1} for the natural sample and 76 mEq 100 g^{-1} for the calcined one.

The PLA and PBAT blend under the trade name Ecovio® from BASF (São Paulo, Brazil) was used as a polymeric matrix. Its properties are defined according to the ratio of each component. Ecovio® F blend C2224 containing 45% PLA and a fusion temperature between 110 and 120 °C were used in this study.

Three ILs were synthesized (name, code, molecular formula): 1-butyl-3-methylimidazolium tetrafluoroborate ($BMIBF_4$) $C_8H_{15}BF_4N_2$; 1-octyl-3-methylimidazolium tetrafluoroborate ($OMIBF_4$) $C_{12}H_{23}BF_4N_2$; 1-dodecyl-3-methylimidazolium tetrafluoroborate ($DMIBF_4$) $C_{16}H_{31}BF_4N_2$. The synthesis was performed in two steps; first, the quaternization of the nitrogen compound from an equimolar mixture of methyl-imidazolium and butyl bromide (purity > 98.0%, acquired from Sigma-Aldrich, São Paulo, Brazil). Octyl bromide or dodecyl bromide (Sigma-Aldrich, São Paulo, Brazil) was used for the other synthesized ionic liquids. The mixture was kept under reflux and stirring at a temperature ranging from 80 to 90 °C for 3 h. At the end of the process, a white solid was formed, then recrystallized with a (1:1) acetonitrile and tetrahydrofuran (THF) mixture (Sigma-Aldrich, São Paulo, Brazil). After recrystallization, all three quaternized compounds presented as a white solid with yielding more than 90%. In the second step, consisting of ion exchange, equimolar amounts of the quaternized compounds and tetrafluoroboric acid (HBF_4) (purity 48.0%, Sigma-Aldrich, São Paulo, Brazil) both dissolved in water, were kept under stirring at room temperature for 1 h, forming a two-phase mixture. The organic phase was extracted in dichloromethane (ACS reagent, Rio de Janeiro, Brazil), the extract eluted on an alumina column, and dried with anhydrous magnesium sulfate (Neon Commercial, Belo Horizonte, Brazil). After that, the dichloromethane was removed by vacuum, generating a slightly yellowish oil as

the final product for $BMIBF_4$ and slightly yellowish solids for $OMIBF_4$ and $DMIBF_4$. The yield for all the synthesized ionic liquids was greater than 70%.

Montmorillonite functionalization

Functionalization of MMT clays was performed by aqueous clay dispersion at a 2% (m/m) concentration in water. The suspension was kept under constant 90 rpm stirring for 2 h at 80 °C. Ionic liquids were added at a 125% (m/m) concentration for the cation exchange capacity of the activated MMT and kept under magnetic stirring for 12 h at 80 °C. The suspension with the functionalized MMTs was centrifuged at 5,000 rpm for 4 min. The solid obtained was dried at 80 °C for 24 h, then deagglomerated manually, and classified on a 200 mesh sieve (74 μm opening).

Polymeric films by casting

The composites were obtained by casting-type molding method, a solubilization technique followed by solvent evaporation that results in polymeric films with the functionalized clays. The matrix solution was then prepared at 50 mg mL^{-1} Ecovio® in chloroform (99% from FMaia, São Paulo, Brazil) that was kept under magnetic stirring for 1 h at a constant temperature until complete dissolution of the polymer. Afterward, the functionalized MMT was added at 2.5 and 5% relative to the polymer mass. The solution was kept under magnetic stirring for 2 h at room temperature. The solutions were placed in 7-cm-diameter non-stick Teflon molds. Solvent removal occurred in an oven at 40 °C for 24 h. Once removed from the discs, the films were wrapped in aluminum foil and stored in a desiccator.

Instrumental methods

The thermogravimetric analyses (TGA), differential thermogravimetric analyses (dTGA), and differential scanning calorimetry (DSC) have been performed in a simultaneous thermal analyzer STA 6000 PerkinElmer (Medianeira, Brazil). For each sample, 10 mg were placed into an open alumina crucible and heated from 50 to 650 °C at a 10 °C min^{-1} heating rate under an inert atmosphere (N_2, White Martins, Brazil, 99.99% grade) and dynamic atmospheres with a 20 cm^3 min^{-1} flow rate.

The X-ray diffractograms (XRD) were obtained using a PANalytical diffractometer (XRD Empyrean model, Foz do Iguaçu, Brazil), operating with a current of 20 mA, voltage of 40 kV, equipped with a copper tube, $K\alpha = 0.15418$ nm, scanning range from 3 to 80°/2θ and scanning speed of 0.02° min^{-1}, using silicon (Si) as internal standard. The diffractograms obtained in the temperature range of 25 to 600 °C were obtained with an internal heating accessory in a carbon dome with a heating rate of 10 °C min^{-1}.

Fourier transform infrared spectra (FTIR) were obtained in the 4000 to 600 cm^{-1} range at room temperature, using the attenuated total reflectance module, with 16 scans accumulation and a 2 cm^{-1} resolution using a PerkinElmer Spectrum 100 (Medianeira, Brazil) equipment.

The mechanical properties tests followed the ASTM D882-02 (Standard Test Method for Tensile Properties of Thin Plastic Sheets). A universal Texturometer model TA.HD Plus Stable Micro Systems (Medianeira, Brazil), was used for the tests. The samples of each formulation were cut 25 mm long and 10 mm wide and adjusted in the equipment. The traction rate used on the composites was 1 mm s^{-1} with an initial 15 mm distance between the grips and 5 kgf was the applied load cell.

Results and Discussion

Natural MMT characterization

The TGA, dTGA and DSC analysis profiles for the natural clay are presented in Figure 1.

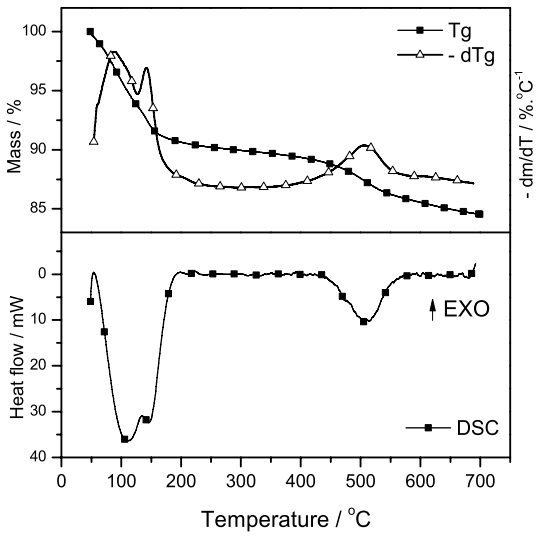

Figure 1. Thermogravimetric (TGA), differential thermogravimetric (dTGA) profiles, and differential scanning calorimetry (DSC) analysis for natural clay.

The natural clay sample exhibited at least three mass loss processes. The first two occurred in overlap and showed a mass change of about 10%, with respective endothermic processes between 50 and 200 °C attributed to thermal events of dehydration and loss of adsorbed moisture. This evaporation is attributed to water found on the inorganic

cations and the aluminosilicate surfaces.[19] The apparent double and overlapping process may be related to the presence of calcium and magnesium installed as cations, resulting in interactions of different intensities between the adsorbed water and clay, or also to the presence of chemical contaminants.[20]

The thermal event near 520 °C, also an endothermic process, is linked to the oxidation or loss of structural hydroxyls.[21] Clays with low iron composition present a thermal event near 700 °C, and in cases of excess Fe, it occurs near 500 °C related to the loss of $Fe(OH)_3$ hydroxyls. The natural clay presented an 85% residual mass at 700 °C.[13]

Considering the thermal analyses information, the need for thermal treatment became evident to eliminate molecules previously adsorbed on the clay. Aiming at a future adsorption process, this treatment cannot occur at temperatures higher than around 400 °C because dehydroxylation of the clay is not a desired event. Thus, 250 °C was established for the calcination/activation of natural clay.

The structural characterization of the clay was performed by the X-ray diffraction technique with diffractograms of natural clay recorded at several temperatures ranging from 25 to 600 °C. The diffractograms are shown in Figure 2.

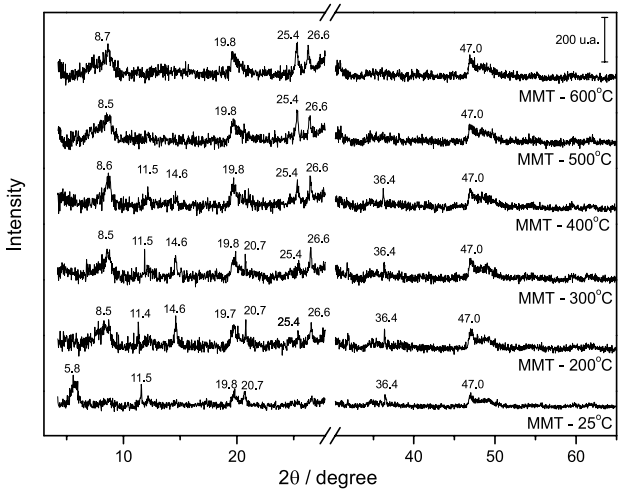

Figure 2. Diffractograms for the natural clay at different temperatures. MMT: montmorillonite.

The diffractogram at room temperature (25 °C) showed that at least one fraction of the clay studied was composed of montmorillonite since its characteristic peak at 2θ of 5.8° was observed, and its intensity is due to interlamellar water or possible intercalating agents (Morita *et al.*).[22] Above 200 °C, moisture loss and a shift of this peak to a higher angle (8.5°) occurred, indicating decreased basal spacing. Comparing the d(001) values for these two peaks, a 0.48 nm compaction in the basal spacing, which went from 1.52 nm natural to 1.04 nm after 200 °C, was noted. At subsequent temperatures for the same peak, there was a low 8.5° and 8.7° variation, indicating constancy in the crystal structure of MMT at temperature and hence the basal spacing.[23]

The diffractogram profile at 200 °C and above usually showed progressive changes in intensities related to changes in the crystallinity of the sample or electrostatically fixed cations and isomorphic replacements in its central octahedral layer by temperature.[11,24] Such changes may be noted by the peak at 14.6°, referring to the dehydration process, and in the peak at 25.4°, attributed to the temperature-proportional increase in crystallinity. These results corroborate with those from heat treatment from 300 to 500 °C in natural MMT.[25,26]

The visible peak at 11.5° is possibly linked to accessory minerals such as kaolinite, which exhibits a dehydroxylation process at 500 °C.[23] In addition, the 20 to 30° range showed peaks linked to accessory minerals such as mica and quartz, which present changes by the structural conformation of the material.[22] For temperatures above 200 °C, the intensity of the apparent peak at 26.6°, attributed to the presence of quartz, increased with increasing temperature. Such changes are due to the heat treatment altering the structure of the clay by the crystal lattice destruction, causing structural rearrangement of the sample and the formation of quartz.[25] After 500 °C, the disappearance of the peaks at 2θ of 11.5°, 14.6°, and 36.4°, referring to MMT dehydroxylation, and total degradation of carbonaceous material was verified, with a vigorous decrease in d(001), indicating the intercalary gallery collapse.[20] The residual peaks in the 600 °C range are attributed to the inorganic material, which maintained their multilayer structure and increased peaks intensity.[27]

Considering the basal spacing reduction, a temperature at which excess moisture and possible chemical contaminants are removed is advantageous. Based on these results and the initial TGA analysis of the natural sample, a thermal activation pre-treatment of MMT at 250 °C was established to provide such removals while avoiding dehydroxylation that may reduce active sites on the MMT surfaces.[18]

Characterization of functionalized MMTs

The results of the XRD, TGA, and FTIR analyses may confirm activated MMT functionalization. The X-ray diffraction profiles in Figure 3, when compared to the active MMT sample, showed that the characteristic peak of clay (8.8°) shifted to smaller angles of 6.5°, 6.2°, and 6.2° for the three ILs with aliphatic chains of 4, 8, and 12 carbons, respectively. This result indicated that the basal spacing of MMT is widened by the methylimidazolium

cations intercalation process.[28] However, the residual peak at 8.8° may indicate a portion of non-intercalated clay. This residual peak may be due to MMT dihydroxylation during heat treatment and deactivating ion-exchange sites.

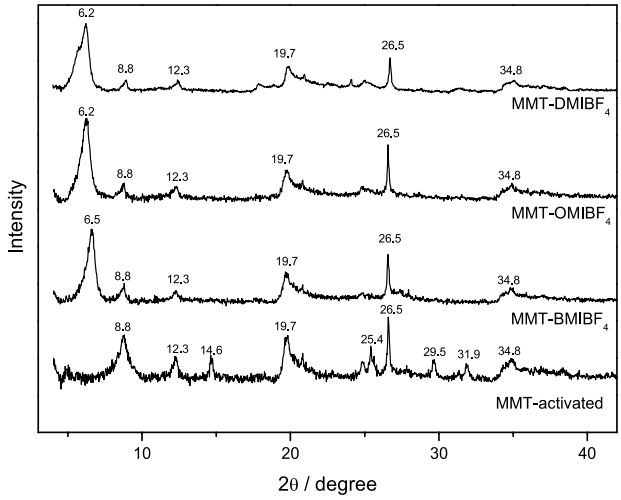

Figure 3. Diffractogram for the natural calcined and functionalized clay samples. MMT: montmorillonite; $BMIBF_4$: 1-butyl-3-methylimidazolium tetrafluoroborate; $OMIBF_4$: 1-octyl-3-methylimidazolium tetrafluoroborate; $DMIBF_4$: 1-dodecyl-3-methylimidazolium tetrafluoroborate.

The peaks at 2θ of 14.6°, 29.5°, and 31.9°, present in the activated MMT diffractogram were not observed in the functionalized samples, indicating the ILs intercalation process in the activated MMT. Intercalation possibly occurs by replacing OH groups for the organic salt, and due to the amorphous character of ionic liquids, no associated signals are expected in the diffractogram. Organic molecules increased the d(001) spacing and decreased the degree of crystallinity of the sample. As for the accessory minerals, peaks at 19.7°, 26.5°, and 34.8° also did not have any relevant modifications in intensity, confirming their secondary character. The peak at 26.5°, visible in the activated MMT and attributed to the arrangement in the crystalline reticulate, had its intensity reduced. However, it was observed in the functionalized samples, allowing us to infer that the heat treatment temperature did not affect the structural pattern of the activated sample.[19,29,30]

Table 1 shows the increase in basal spacings d(001), calculated by Bragg's Law, which allowed us to infer that the imidazolium cations from the IL replaced the exchangeable calcium ions from the clay. Furthermore, from the ratio of the values, it was assumed that the alkyl groups are organized into a monolayer parallel structure in the MMT-$BMIBF_4$ sample galleries.[31] The shifts were not proportional to the number of carbons in the alkyl chain of IL; since the MMT-$OMIBF_4$ and MMT-$DMIBF_4$ samples showed similar values. It demonstrates that the parallel monolayer structure was maintained. Such fact may be linked to the low cation exchange capacity (CEC) of the clay studied that allows the accommodation of alkyl chains in parallel with the MMT lamellae.

Table 1. Functionalization results in the basal spacing of clay samples 4, 8, and 12

Sample	Alquil chain	2θ / degree	Basal spacing / nm
Natural-MMT	–	5.8	1.54
Activated-MMT	–	8.8	1.00
MMT-$BMIBF_4$	4	6.5	1.36
MMT-$OMIBF_4$	8	6.2	1.41
MMT-$DMIBF_4$	12	6.2	1.42

MMT: montmorillonite; $BMIBF_4$: 1-butyl-3-methylimidazolium tetrafluoroborate; $OMIBF_4$: 1-octyl-3-methylimidazolium tetrafluoroborate; $DMIBF_4$: 1-dodecyl-3-methylimidazolium tetrafluoroborate.

There was a pseudo-bilayer conformation for these samples, mainly due to the low CTC of natural MMT. The expected increase in d(001) occurred due to the angulation generated in the carbon chains and their length and concentration. However, there was no tendency to perpendicular or paraffinic arrangements in the interlamellar space as the carbon chain increased. Possibly the chains curved during intercalation due to the pressure between the galleries exceeding that of the environment at low CTC conditions.[32]

Evidence of MMT functionalization by ILs was sought from infrared spectroscopy. Figure 4 shows the FTIR spectra of activated MMT and the MMT-ILs. The bands between 3200 and 3100 cm^{-1} were assigned to stretching vibration of C=C–H and N=C–H bonds in the imidazolium rings and present at low intensity in the functionalized MMT spectra. As the ILs carbon chain increased, a decrease in the intensity of the bands related to stretching OH from hydroxylated surface residues that the ILs replaced was observed. It is believed that this effect is caused by increased MMT-IL hydrophobicity when functionalized by longer carbon chain ILs.[12,30]

The bands in the range of 3000 and 2800 cm^{-1} and at 1470 cm^{-1} are characteristic, respectively, of symmetric and asymmetric $–CH_2–$ methylene groups stretching of the hydrocarbon chains of ionic liquids and of the bending vibration of imidazolium-based organic groups, reasserting the ionic liquids intercalation into the MMT layers.[17] The band around 1630 cm^{-1} in the MMT-calcinate spectrum was attributed to the bending vibration of the H–O–H water molecules absorbed by the silicate, and its reduction in MMT-IL cases demonstrates the increased hydrophobicity of the functionalized clay.

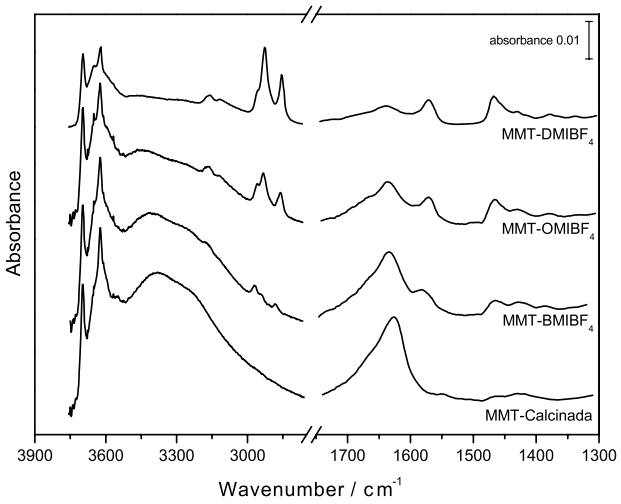

Figure 4. Fourier transform infrared spectra (FTIR) with detail for characteristic bands of the organic solvents. MMT: montmorillonite; $BMIBF_4$: 1-butyl-3-methylimidazolium tetrafluoroborate; $OMIBF_4$: 1-octyl-3-methylimidazolium tetrafluoroborate; $DMIBF_4$: 1-dodecyl-3-methylimidazolium tetrafluoroborate.

The shift of methylene groups from 2970 cm^{-1} in MMT-$BMIBF_4$ to 2928 cm^{-1} in MMT-$OMIBF_4$ and MMT-$DMIBF_4$, i.e., to lower frequency regions, indicates higher ordering. In addition to the lateral monolayer structure, it was also found with carbon chain increase a tendency to a solid-like *trans* arrangement. Although it presents easy cation exchange and is suitable for industrialization, the more stable solid-state may be disadvantageous to the composition with polymer.[14,33]

The thermogravimetric and differential thermogravimetric profiles of functionalized clays with different carbon chain sizes are shown in Figure 5. For all samples, a first thermal dehydration event was observed that ended before 150 °C and after that, a second mass loss related to the degradation of carbon chains in two phases that begins close to 550 °C.[12,14] In this degradation range, the first phase started after 250 °C. It corresponds to molecules adsorbed on the outer surface of the lamellae or molecules with SiOH interactions in peripheral positions at the edges of the layers.[20] The second phase of mass loss, visible near 500 °C, corresponds to the IL species intercalated between the silicate layers.[7,16] The disappearance of the initial double peak visible in MMT calcined at 100 °C may be due to the replacement of the calcium and magnesium cations in the natural sample by organic IL groups.

The sample MMT-$BMIBF_4$ was the most thermally stable among the functionalized clays, having the onset of thermal degradation at approximately 390 °C. For the MMT-$OMIBF_4$ and MMT-$DMIBF_4$ samples, degradation temperatures of 355 and 335 °C were respectively observed, demonstrating that the increase in the carbon chain affected the thermal stability of the clay. For the residual mass, sample MMT-$BMIBF_4$ showed the highest residual mass (91%). The residual masses of MMT-$OMIBF_4$ and MMT-$DMIBF_4$ samples were 89 and 83%, respectively, and 93% residual mass for MMT. This was expected since the IL mass is higher for larger chains. These results are in agreement with studies by Pucci *et al.*[12] for alkyl-imidazolium salts, where thermal stability decreases with the increase in carbon atoms in the chain.

PBAT/PLA and IL-MMT composite films characterization

The MMT functionalized with ILs were incorporated into the PBAT/PLA blends by casting technique, creating composite films with 2.5 and 5% MMT-IL by mass. The effect of MMT-IL addition on the composites was observed regarding the structural characteristics with the X-ray diffraction technique, the thermal behavior by

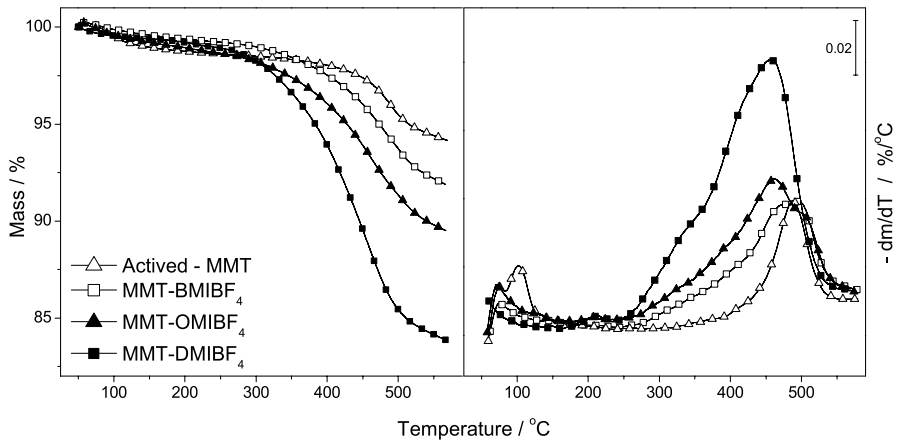

Figure 5. Thermal decomposition and mass change as a function of temperature curves for the calcined and functionalized MMT samples. MMT: montmorillonite; $BMIBF_4$: 1-butyl-3-methylimidazolium tetrafluoroborate; $OMIBF_4$: 1-octyl-3-methylimidazolium tetrafluoroborate; $DMIBF_4$: 1-dodecyl-3-methylimidazolium tetrafluoroborate.

thermogravimetry, and the mechanical properties by tensile analysis.

X-ray diffraction analysis was performed to evaluate the effect of MMT-IL addition on the structural characteristics of the composites produced. The diffractograms in Figure 6 showed the dispersion and exfoliation of MMT-ILs by analyzing the position, shape, and intensity of the basal reflections of the silicate layers.[1] The activated MMT presented a peak at 8.8°, and the MMT-ILs presented peaks near 6°. The diffractogram of the composites showed that total exfoliation of MMT-IL for Ecovio-MMT and Ecovio-MMT-$BMIBF_4$ films occurred due to the disappearance of the characteristic peaks of the clay, the separation of the MMT-IL layers, and the favorable interactions with the PLA/PBAT blends. Hence, there are indications of exfoliated nanocomposites formation.[3]

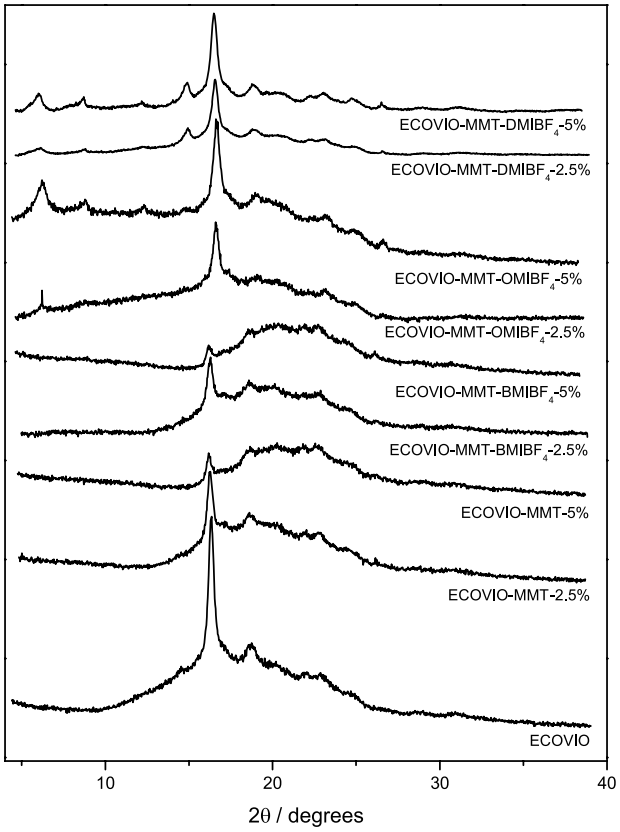

Figure 6. Diffractograms for Ecovio films with MMT-IL samples 5% by mass. MMT: montmorillonite; IL: ionic liquids; $BMIBF_4$: 1-butyl-3-methylimidazolium tetrafluoroborate; $OMIBF_4$: 1-octyl-3-methyl-imidazolium tetrafluoroborate; $DMIBF_4$: 1-dodecyl-3-methylimidazolium tetrafluoroborate.

The characteristic peaks of MMT-IL for Ecovio-MMT-$OMIBF_4$ and Ecovio-MMT-$DMIBF_4$ remained in the diffractogram of the composite films, indicating no MMT-IL dispersion. The changes in peak widths and intensities confirmed the polymer matrix-MMT-IL interaction. In this case, however, the clay layers maintained their stacking since their peaks did not present shifts 2θ smaller, thus inferring that no increase in the basal distance by the PLA/PBAT blend intercalation into the interlamellar spaces occurred. Thus, suggesting micro composites formation.[12,34]

The PBAT/PLA blend presents moderately polar groups and, therefore, showed better interaction with the 4-carbon chain and also with the non-functionalized clay that presents a hydrophilic surface. Even though ionic liquids present amphiphilic character, MMT-$OMIBF_4$ and MMT-$DMIBF_4$ samples became more hydrophobic due to the increase in hydrophobicity of the MMT-IL samples as the number of carbons in the IL chain increases.[35] It may be verified by the increased intensity peak at 16° in the samples, characteristic of PLA, whose increase in intensity is directly linked to the increased crystallinity of the dispersed phase.

For PLA crystallinity, the diffractogram of the pure film showed that the blend presents high crystallinity of this component. Crystallinity in Ecovio-MMT and Ecovio-MMT-$BMIBF_4$ films was reduced due to the polarity of the natural clay and the imidazolium cation that allowed favorable interactions with the carbonyl group found in the PLA polymer chain.[35] Evaluating the noticeable decrease in the intensity of the characteristic peak of PLA in Ecovio-MMT and Ecovio-MMT-$BMIBF_4$ films, a similar degree of reduction in the crystallinity of the film was noted due to the exfoliated-MMT platelets disorder.

For the Ecovio-MMT-$OMIBF_4$ and Ecovio-MMT-$DMIBF_4$ films, the shift of the PLA main peak was caused by the decrease in the number of polymer chains to be intercalated and also to the increased stacking of intercalated silicate layers. The band between 15 to 25°, referring to the PBAT crystalline phase in the blend, showed similar interaction in Ecovio-MMT and Ecovio-MMT-$BMIBF_4$ films. Such phase for the Ecovio-MMT-$OMIBF_4$ film was softened, suggesting an IL and PBAT interaction.

As for the MMT-IL content increase in the composite films, it was noted that in the Ecovio-MMT and Ecovio-MMT-BMIBF4 samples, where MMT-IL exfoliation occurred, the content increase led to crystallinity decrease caused by the reduction of crystalline domains by the greater MMT-IL dispersion in the polymer matrix. For the Ecovio-MMT-$OMIBF_4$ and Ecovio-MMT-$DMIBF_4$ samples that generate micro composites, the increase in MMT-IL content lead to clay agglomeration increasing crystallinity linked to MMT.

The thermogravimetric and differential thermogravimetric analyses of pure blends and composite films are presented in Figure 7.

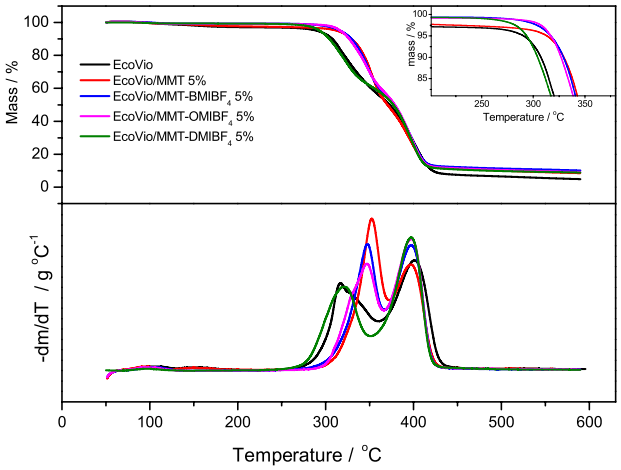

Figure 7. Thermogravimetric curves for pure poly (butylene adipate co-terephthalate)/polyester poly (lactic acid) (PBAT/PLA) blend films and MMT-IL composites at a 5% (m/m) ratio. MMT: montmorillonite; IL: ionic liquids; $BMIBF_4$: 1-butyl-3-methylimidazolium tetrafluoroborate; $OMIBF_4$: 1-octyl-3-methylimidazolium tetrafluoroborate; $DMIBF_4$: 1-dodecyl-3-methylimidazolium tetrafluoroborate.

As it is an immiscible blend, the thermogravimetric profile of the Ecovio film presents at least two mass loss processes referring to the individual decomposition of each polymer; the first with a maximum at around 315 °C corresponding to PLA degradation and the second one with maximum degradation at about 400 °C referring to PBAT.[36]

Evaluating the thermal behavior of composites with MMT and MMT-IL compared to that of pure blends, it was noted that the mass loss phases for Ecovio-MMT, Ecovio-MMT-$BMIBF_4$, and Ecovio-MMT-$OMIBF_4$ samples presented the first process shifted to higher temperatures, with a maximum at around 350 °C. This shift is due to favorable interactions between the exfoliated MMT-IL and, specifically, the polymeric fraction of the PLA. Even though the XRD analysis showed no exfoliation of the Ecovio-MMT-OMIBF4 sample, in this case, it showed good interaction with the polymer.

The Ecovio-MMT-$DMIBF_4$ sample showed a thermogravimetric profile similar to that observed for the pure Ecovio film. This is due to the high carbon chain present in the IL, making the modified clay surface with very low polarity, not favoring the clay and polymer matrix interaction. These observations were consistent with those from Ha *et al.*,[17] who described composites where the MMT-IL was exfoliated in a polypropylene matrix, i.e., nanocomposites exhibit superior thermal stability than composites where MMT-IL does not present any exfoliation (defined as micro composites). Moussout *et al.*[37] concluded that thermal stability increases in the chitosan/bentonite composite occurred due to the strong synergistic effect between the clay and the polymer matrix, a behavior similar to that observed in this present study.

Figure 7 shows the three samples that presented some degree of intercalation, despite their different levels of interaction; MMT, butyl, and octyl, whose thermal stability increased with increasing the MMT-IL loading. In their study with PLA and MMT functionalized with phosphonium-based IL, Alves *et al.*[15,38] identified a considerable decrease in the initial thermal degradation

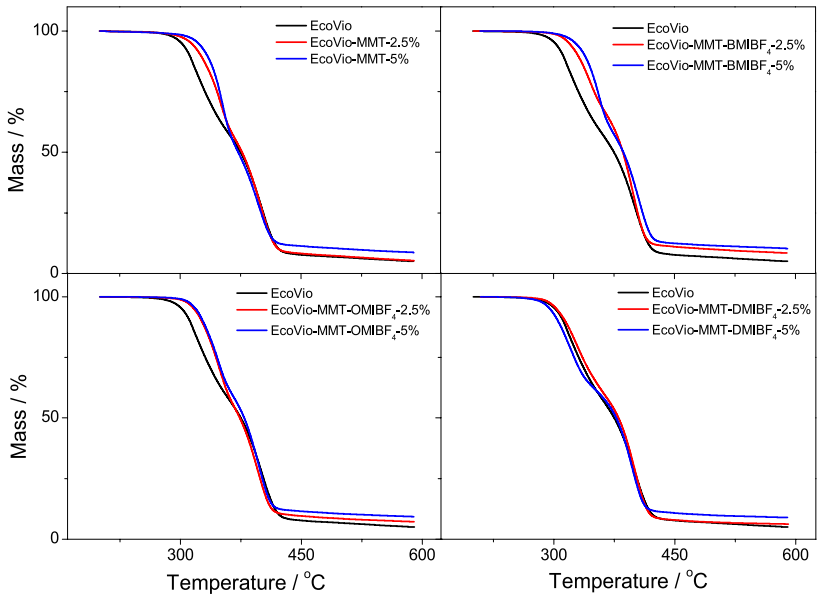

Figure 8. Thermogravimetric curves for the 2.5 and 5% MMT-IL (m/m) composite films. MMT: montmorillonite; IL: ionic liquids; $BMIBF_4$: 1-butyl-3-methylimidazolium tetrafluoroborate; $OMIBF_4$: 1-octyl-3-methylimidazolium tetrafluoroborate; $DMIBF_4$: 1-dodecyl-3-methylimidazolium tetrafluoroborate.

temperature and continuously as the load increased. Contrary to such results, imidazolium-based IL showed better performance since the chemical composition of the silicates affects the thermal stability.

For other curves, dodecyl, compared to the behavior of pure blend, the mass loss phases were very close to the pure blend curve, consistent with the micro composites conformation.[37,39] For the 5% content, the Ecovio-MMT-DMIBF$_4$ film reduced the thermal stability of the blend. Increasing the MMT-IL content increased the density of clay-rich regions in the composite, causing a higher heat flow, thus accelerating the degradation process.[40]

For the mechanical behavior of the composite films, it was evaluated that MMT-IL caused considerable effects on the PBAT/PLA blend film. Table 2 presents the modulus of elasticity or Young's modulus, rupture strain, maximum applied stress for each sample, and the pure Ecovio film. For the modulus of elasticity, the samples, except Ecovio-MMT-2.5%, Ecovio-MMT-DMIBF$_4$-2.5%, and Ecovio-MMT-DMIBF$_4$-5%, showed a higher modulus of elasticity when compared to the film not added with MMT and MMT-IL.

The Ecovio-MMT-BMIBF$_4$-2.5% film presented the best performance for modulus of elasticity, a relevant fact considering the low content of MMT-IL and the accentuated effect on the modulus of elasticity. Such effect may be related to nanoscale interactions due to MMT-IL exfoliation, as described by Paul and Robeson.[6] The advanced stage of interactions between MMT-IL and the polymer matrix caused marked changes in material properties, such as improved stiffness.[34] The increase in the modulus of elasticity of the Ecovio-MMT-BMIBF$_4$-2.5% sample was 58% when compared to the Ecovio film. Similar results were observed by Livi *et al*.,[7] who obtained a 40% increase in the modulus of elasticity of polyethylene in a composite with exfoliated MMT-IL. Lim *et al*.,[40] when analyzing biodegradable polyester and montmorillonite composite, observed that fine dispersions of non-exfoliated organophilized MMT particles also improved the modulus of elasticity by forming micro composites. The other samples produced had a lower degree of interaction between polymer matrix and MMT-IL. Therefore, the micro composites profile is more suitable, even more so considering that the XRD results showed evidence of remaining crystalline structure in Ecovio-MMT-OMIBF$_4$ and Ecovio-MMT-DMIBF$_4$ samples.

The Ecovio-MMT-2.5% sample showed, besides a low load content that may not be enough to increase final properties, a reduction in its modulus may be linked to the lower blend silicate sheets surface interaction.[34] For 5% content, the improvement was more directly linked to the load concentration in the film than to the MMT-IL and the polymeric matrix interaction. In this context, Majka *et al*.[8] limit such contents to 5% since the possible collapse of the bonds between the silicate and the polymeric matrix generates greater fragility and cracks on the composite surface. The authors justified that the increased content causes MMT agglomeration and, consequently, mechanical properties reduction.

For films containing MMT-DMIBF$_4$, the modulus of elasticity was slightly lower than that observed for the pure Ecovio film. Such effect may be attributed to silicates agglomeration generated by the long dodecyl chains and accentuated by the increased MMT-IL contents. Araújo *et al*.[41] observed a reduction in the modulus of elasticity by adding MMT-OMIBF$_4$ in the PBAT/PLA blend and justified it by the low micro composites interaction and formation. Alexandre and Dubois[34] also reported that the increase in intensities in XRD diffractograms was inversely related to the number of exfoliated layers in the nanocomposite and the decrease in Young's modulus in the

Table 2. Tensile analysis results for Ecovio film obtained by casting method

Sample	Modulus of elasticity / MPa	Strain at break / %	Tensile strength / MPa
Ecovio	315 ± 50	4.04 ± 0.50	5.55 ± 1.74
Ecovio-MMT-2.5%	270 ± 50	3.31 ± 0.12	6.37 ± 1.62
Ecovio-MMT-5%	346 ± 60	3.71 ± 0.36	7.67 ± 1.24
Ecovio-MMT-BMIBF$_4$-2.5%	487 ± 30	4.98 ± 0.41	13.81 ± 2.23
Ecovio-MMT-BMIBF$_4$-5%	435 ± 20	2.98 ± 0.45	8.77 ± 0.31
Ecovio-MMT-OMIBF$_4$-2.5%	393 ± 40	3.36 ± 0.60	7.90 ± 1.72
Ecovio-MMT-OMIBF$_4$-5%	312 ± 30	2.42 ± 0.32	6.43 ± 0.75
Ecovio-MMT-DMIBF$_4$-2.5%	305 ± 40	2.15 ± 0.50	5.65 ± 0.60
Ecovio-MMT-DMIBF$_4$-5%	295 ± 30	1.85 ± 0.41	5.43 ± 0.80

MMT: montmorillonite; BMIBF$_4$: 1-butyl-3-methylimidazolium tetrafluoroborate; OMIBF$_4$: 1-octyl-3-methylimidazolium tetrafluoroborate; DMIBF$_4$: 1-dodecyl-3-methylimidazolium tetrafluoroborate.

sample. Such facts corroborate the assumption of micro compositions in Ecovio-MMT-DMIBF$_4$ films for both the studied contents.

For the complementary results for strain and maximum tensile, the degree of dispersion exerted similar effects on such parameters. Intrinsically linked to this fact, the strain capacity of films, except for the Ecovio-MMT-BMIBF$_4$-2.5% one, presented lower behavior to the natural blends. For the filler ratios, films containing natural MMT exhibited opposite behavior to MMT-IL, which showed lower results for higher clay concentrations in the pairwise comparison. Similar links were verified for tensile strength. Araújo *et al*.[41] also concluded for all the systems analyzed that low filler contents generate improved mechanical properties, both tensile strength and modulus of elasticity.

Conclusions

Composites were prepared between poly (butylene adipate *co*-terephthalate) / poly (lactic acid) (PBAT/PLA) polymer blend and montmorillonite (MMT) functionalized with three alkyl-imidazolium ionic liquids (ILs) of different alkyl chain sizes (butyl, octyl, and dodecyl). The composites were prepared by the casting method generating homogeneous films.

The functionalization of the montmorillonite was proven by increasing interlamellar spacing in the three MMT-IL samples. However, this widening was not proportionate to the size of the butyl, octyl, and dodecyl carbon chains of the ILs. Larger alkyl chains promote and intensify disordered conformation, and, therefore, the d(001) values did not follow the increasing proportion.

For the composite films, the addition of 2.5 and 5% MMT-IL showed changes in the mechanical tests for all films and also affected the thermal properties of the material.

As a main result, the mechanical and thermal properties improvement shown by the Ecovio-MMT-BMIBF$_4$ film was indicated. For the mechanical properties, the modulus of elasticity increased 58% when compared to the PLA/PBAT blends. The thermal stability of the material also showed a considerable increase in this composition. Such effect is related to the possible exfoliation of the material and the formation of a more structurally homogeneous composite.

At last, it may be stated that the PBAT/PLA blend, commercially found as Ecovio™, may improve their thermal and mechanical properties by adding natural MMT functionalized with alkyl-imidazolium-based ionic liquids.

Acknowledgments

The authors are grateful for the financial support provided by the Brazilian research funding agencies CAPES and CNPQ, and Central Analítica Mulltiusuário da Universidade Tecnológica Federal do Paraná (CEANMED/ Campus Medianeira, Paraná State, Brazil), by the assays performed.

Author Contributions

Renata S. Dias was responsible for experimental, conceptualization, methodology, data collection; Fernando R. Scremin for experimental, conceptualization, methodology, data collection, writing original draft, results analysis; Paulo R. S. Bittencourt for data collection, results analysis, writing (review and editing); Douglas C. Dragunski for writing (review and editing), results analysis; Alex S. Torquato for results analysis, writing (review and editing); Oldair D. Leite for funding acquisition, conceptualization, supervision, methodology, results analysis, writing (review and editing).

References

1. Sinharay, S.; Bousmina, M.; *Prog. Mater. Sci.* **2005**, *50*, 962. [Crossref]
2. Siegenthaler, K. O.; Künkel, A.; Skupin, G.; Yamamoto, M. In *Synthetic Biodegradable Polymers*; Rieger, B.; Künkel, A.; Coates, G.; Reichardt, R.; Dinjus, E.; Zevaco, T., eds.; Springer: Berlin, 2011, ch. 4. [Crossref]
3. Shahlari, M.; Lee, S.; *Polym. Eng. Sci.* **2012**, *52*, 1420. [Crossref]
4. Falcão, G. A. M.; Vitorino, M. B. C.; Almeida, T. G.; Bardi, M. A. G.; Carvalho, L. H.; Canedo, E. L.; *Polym. Bull.* **2017**, *74*, 4423. [Crossref]
5. Tri Phuong, N.; Gilbert, V.; Chuong, B.; *J. Reinf. Plast. Compos.* **2008**, *27*, 1983. [Crossref]
6. Paul, D. R.; Robeson, L. M.; *Polymer* **2008**, *49*, 3187. [Crossref]
7. Livi, S.; Duchet-Rumeau, J.; Pham, T. N.; Gérard, J. F.; *J. Colloid Interface Sci.* **2010**, *349*, 424. [Crossref]
8. Majka, T. M.; Bartyzel, O.; Raftopoulos, K. N.; Pagacz, J.; Leszczyńska, A.; Pielichowski, K.; *J. Anal. Appl. Pyrolysis* **2016**, *119*, 1. [Crossref]
9. Wang, J.; Su, X.; Mao, Z.; *Polym. Degrad. Stab.* **2014**, *109*, 154. [Crossref]
10. Koutroulis, A. G.; *Sci. Total Environ.* **2019**, *655*, 482. [Crossref]
11. Teixeira-Neto, E.; Teixeira-Neto, A. A.; *Quim. Nova* **2009**, *32*, 809. [Crossref]
12. Pucci, A.; Liuzzo, V.; Melai, B.; Pomelli, C. S.; Chiappe, C.; *Polym. Int.* **2012**, *61*, 426. [Crossref]
13. de Paiva, L. B.; Morales, A. R.; Díaz, F. R. V.; *Cerâmica* **2008**, *54*, 213. [Crossref]

14. Kim, N. H.; Malhotra, S. V.; Xanthos, M.; *Microporous Mesoporous Mater.* **2006**, *96*, 29. [Crossref]
15. Alves, J. L.; Rosa, P. T. V. E.; Morales, A. R.; *Mater. Chem. Phys.* **2018**, *218*, 279. [Crossref]
16. Bell, G.; Goss, M.; *Appl. Clay Sci.* **2004**, *27*, 179. [Crossref]
17. Ha, J. U.; Xanthos, M.; *Polym. Compos.* **2009**, *30*, 534. [Crossref]
18. Awad, W. H.; Gilman, J. W.; Nyden, M.; Harris, R. H.; Sutto, T. E.; Callahan, J.; Trulove, P. C.; DeLong, H. C.; Fox, D. M.; *Thermochim. Acta* **2004**, *409*, 3. [Crossref]
19. Khalaf, A. I.; Hegazy, M. A.; *High Perform. Polym.* **2013**, *25*, 115. [Crossref]
20. Xie, W.; Gao, Z.; Liu, K.; Pan, W. P.; Vaia, R.; Hunter, D.; Singh, A.; *Thermochim. Acta* **2001**, *367-368*, 339. [Crossref]
21. Xie, W.; Xie, R.; Pan, W. P.; Hunter, D.; Koene, B.; Tan, L. S.; Vaia, R.; *Chem. Mater.* **2002**, *14*, 4837. [Crossref]
22. Morita, R. Y.; Barbosa, R. V.; Kloss, J. R.; *Rev. Virtual Quim.* **2015**, *7*, 1286. [Link] accessed in July 2024
23. Morodome, S.; Kawamura, K.; *Clays Clay Miner.* **2011**, *59*, 165. [Crossref]
24. Leszczyńska, A.; Njuguna, J.; Pielichowski, K.; Banerjee, J. R.; *Thermochim. Acta* **2007**, *454*, 1.[Crossref]
25. Garg, N.; Skibsted, J.; *J. Phys. Chem. C* **2014**, *118*, 11464. [Crossref]
26. Zuo, Q.; Gao, X.; Yang, J.; Zhang, P.; Chen, G.; Li, Y.; Shi, K.; Wu, W.; *J. Taiwan Inst. Chem. Eng.* **2017**, *80*, 754. [Crossref]
27. Güler, Ç.; Sarier, N.; *Thermochim. Acta* **1990**, *159*, 29. [Crossref]
28. Karakehya, N.; Bilgiç, C.; *Int. J. Adhes. Adhes.* **2014**, *51*, 140. [Crossref]
29. Takahashi, C.; Shirai, T.; Fuji, M.; *Mater. Chem. Phys.* **2012**, *135*, 681. [Crossref]
30. Xiao, F.; Yan, B.; Zou, X.; Cao, X.; Dong, L.; Lyu, X.; Li, L.; Qiu, J.; Chen, P.; Hu, S.; Zhang, Q.; *Colloids Surf., A* **2020**, *587*, 124311. [Crossref]
31. Hu, Z.; He, G.; Liu, Y.; Dong, C.; Wu, X.; Zhao, W.; *Appl. Clay Sci.* **2013**, *75-76*, 134. [Crossref]
32. Guan, B. Y.; Yu, X. Y.; Wu, H. B.; Lou, X. W. D.; *Adv. Mater.* **2017**, *29*, 1703614. [Crossref]
33. Akpomie, K. G.; Dawodu, F. A.; *J. Taibah Univ. Sci.* **2014**, *8*, 343. [Crossref]
34. Alexandre, M.; Dubois, P.; *Mater. Sci. Eng., R* **2000**, *28*, 1. [Crossref]
35. Ding, Y.; Zhang, C.; Luo, C.; Chen, Y.; Zhou, Y.; Yao, B.; Dong, L.; Du, X.; Ji, J.; *e-Polym.* **2021**, *21*, 234. [Crossref]
36. de Paula, E. L.; Mano, V.; *Quim. Nova* **2012**, *35*, 1084. [Crossref]
37. Moussout, H.; Ahlafi, H.; Aazza, M.; Amechrouq, A.; *Thermochim. Acta* **2018**, *659*, 191. [Crossref]
38. Alves, J. L.; Rosa, P. T. V.; Realinho, V.; Antunes, M.; Velasco, J. I.; Morales, A. R.; *Appl. Clay Sci.* **2019**, *180*, 105186. [Crossref]
39. Moussout, H.; Ahlafi, H.; Aazza, M.; Amechrouq, A.; *Thermochim. Acta* **2018**, *668*, 169. [Crossref]
40. Lim, S. T.; Hyun, Y. H.; Choi, H. J.; Jhon, M. S.; *Chem. Mater.* **2002**, *14*, 1839. [Crossref]
41. Araújo, E. M.; de Melo, T. J. A.; de Oliveira, A. D.; Araújo, H. L. D.; Araújo, K. D.; Barbosa, R.; *Polimeros* **2006**, *16*, 38. [Crossref]

Submitted: January 19, 2024
Published online: August 7, 2024